DESIGN AND EXPERIMENT OF ENERGY FEEDBACK UNIT FOR 15 kV/15 kA AMD EXCITATION PULSE SOURCE*

Z. Zhong, F.-L. Shang†,Ch. liu‡, L. Shang, W. Hu
University of Science and Technology of China, Hefei, China

Abstract

Abstract: The Super Tau-Charm Facility (STCF), a next-generation electron-positron collider led by the University of Science and Technology of China, necessitates a high-quality positron source to sustain continuous operation with high luminosity. The Adiabatic Matching Device (AMD) serves as a critical component for focusing positrons produced by electron bombardment, requiring its excitation pulse source to deliver a peak current of ≥ 15 kA and a pulse rise time of ≤ 3.5 µs. To mitigate the significant power dissipation of the pulse discharge system, an energy feedback circuit was designed. According to the simulation results, the optimized system achieved a dramatic reduction in losses, with the input power reduced by 75% under the condition of the same output power, while enhancing long-term operational stability. This paper elaborates on the power loss simulation of the AMD excitation pulse source, as well as the design and simulation of the energy feedback circuit.

Key words: excitation pulse power for AMD; power loss; energy feedback; photoconductive semiconductor switch

INTRODUCTION

Electron-positron colliders are vital tools for high energy physics research, A high-quality positron source is critical for the high luminosity of the STCF [1]. The STCF plans to use a 2.5 GeV electron beam to bombard a 15 mm tungsten target to generate positrons [2]. This approach generates a positron beam with small transverse dimensions and high current but suffers from significant divergence, making direct acceleration challenging [3]. Positrons produced by electron-tungsten target collisions require focusing by a high-pulse magnet, commonly referred to as Adiabatic Matching Device (AMD), to match the aperture of the capture structure [4]. As shown in Fig. 1, the AMD is a copper pulsed solenoid featuring a tapered inner bore and constant outer diameter, which requires a fast kA-level high-current pulse for operation. The AMD generates a strong magnetic field at the magnet entrance to enable positron focusing. consequently, the AMD and its excitation source are indispensable components of the positron source.

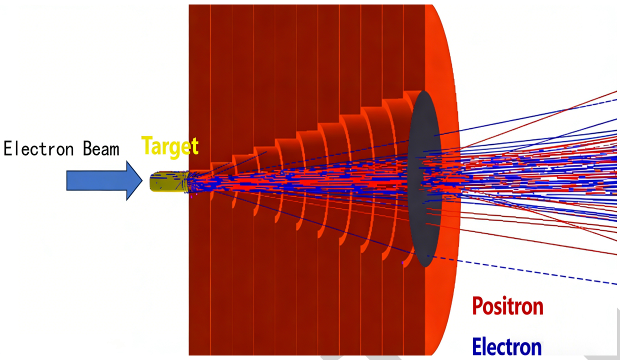

Figure 1: Schematic of the AMD Structure.

Excitation pulse sources, a branch of pulse power technology, rapidly release energy stored in capacitive and inductive components to generate a specific current waveform across the load, thereby achieving energy compression and power amplification [5]. These sources are primarily utilized to provide driving currents for various high-pulse magnet systems in accelerators to enable the focusing, deflection, or confinement of particle beams.

In this study, the RLC series configuration was selected for discharge to generate the current. To suppress the post-pulse oscillation, an energy feedback circuit is proposed in this paper, which reduces power loss and enhances the long-term operational stability of the excitation pulse source.

EXCITATION PULSE SOURCE SCHEME

Two primary discharge method are employed in excitation pulse sources: the RLC series discharge configuration, which generates a half-sine wave; and the Pulse Forming Line (PFN) or Pulse Forming Network (PFL), which produce square-wave pulse currents. Although PFN and PFL schemes are also applicable in some high-voltage conditions, their circuit structures are relatively more complex, and they are usually only adopted in applications that require a long flat-top pulse [6]. So we select RLC series discharge configuration of this excitation pulse source, the parameters are shown in Table 1.

Table 1: Technical Parameters of Excitation Pulse Source

Technical Index	Parameter Requirement
Pulse Current Waveform	Half-Sine Wave
Peak Pulse Current	≥ 15 kA
Pulse Width	5 ± 0.5 µs
Pulse Rise Time	≤ 3.5 µs
Repetition Frequency	50 Hz
Pulse Amplitude Stability	± 0.5%
Peak Charging Voltage	≤ 15 kV
Time Jitter	± 20 ns

---

* We thank the Hefei Comprehensive National Science Center for their strong support on the STCF key technology research project. This work is supported by the National Key R&D Program of China under Contract No. 2022YFA1602200 and the international partnership program of the Chinese Academy of Sciences Grant No. 211134KYSB20200057.

† shangfl@ustc.edu.cn

‡ chaoliu@ustc.edu.cn

Design of Main Discharge Circuit

The main circuit adopts the RLC series circuit discharge principle. According to the equivalent circuit, the differential equation of the discharge circuit is established as follows:

$$LC\frac{d^2i}{dt^2} + RC\frac{di}{dt} + i = C\frac{du_0}{dt} \tag{1}$$

Where, C represents the capacitance of the energy storage capacitor; L represents the total inductance of the circuit (1.8 uH); and R represents the total resistance of the circuit (60 mΩ).

The solution of the current exhibits multiple operating modes, which are determined by the damping coefficient γ ($\gamma = \frac{R}{2}\sqrt{\frac{C}{L}}$).

Ten capacitors of 0.225 µF each were connected in parallel to form the energy storage bank, resulting in a damping coefficient γ between 0 and 1. Therefore, the circuit operates in the underdamped oscillation mode. The peak current and rise time can be derived as follows:

$$I_{peak} = \frac{u_0}{\sqrt{\frac{L}{C} - \left(\frac{R}{2}\right)^2}} e^{-\frac{\gamma}{\sqrt{1-\gamma^2}} \arctan\left(\frac{\sqrt{1-\gamma^2}}{\gamma}\right)} \tag{2}$$

$$t_r = \frac{\arctan\left(\frac{\sqrt{1-\gamma^2}}{\gamma}\right)}{\sqrt{\frac{1}{LC} - \left(\frac{R}{2L}\right)^2}} \tag{3}$$

Selection of Main Switch and Diode

We selected four photoconductive thyristors JLTSU4S-5001D developed by Hubei Jingmai Science and Technology Co., Ltd., which satisfy the high-voltage (15 kV) and high-current (15.5 kA) requirements of the circuit. Simulations were carried out based on their electrical parameters.

SIMULATION AND ANALYSE OF ABSORPTION CIRCUIT

The output excitation pulse current exhibits an underdamped response. For the AMD, only the current peak from the first pulse is utilized, auxiliary circuits are required to eliminate subsequent pulse currents.

The conventional approach involves adding an absorption circuit, composed of a diode and absorption resistor, to the capacitor, as shown in Fig. 2. After the load current reaches its peak, the capacitor enters a reverse charging state, triggering diode conduction and dissipating the load energy through the absorption resistor.

The simulation utilize a 2 Ω absorption resistor. Calculations indicate that the total energy input to the energy storage capacitor per pulse is approximately 253 J, of which 195 J is dissipated through the absorption resistor, only 18 J is utilized by the AMD load, resulting in an energy utilization efficiency of merely 7.11%. Excessive heat from absorption resistor substantially increase the failure rate of semiconductors, thereby imposing stringent demands on the cabinet heat dissipation system.

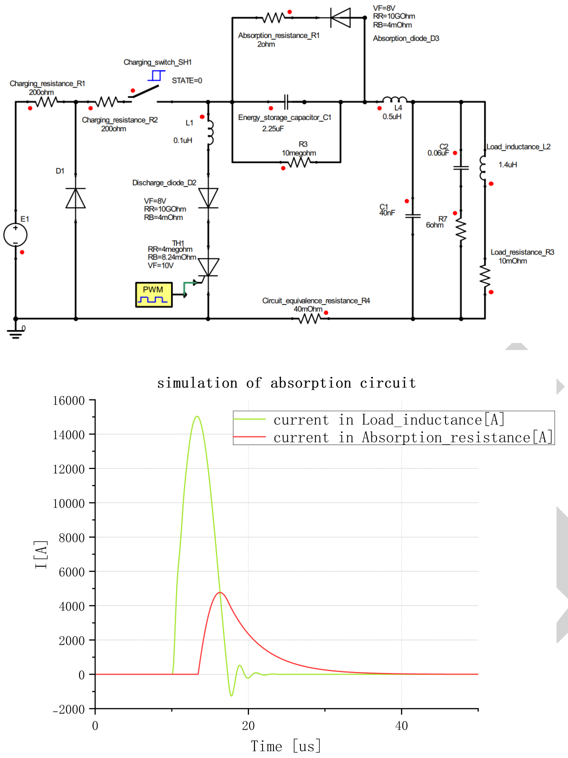

a)

b)

Figure 2: Simulation of the absorption circuit. (a) Simulation diagram. (b) Simulated results.

For fan-based cabinet heat dissipation, the relationship between heat generation and air volume is described by the following equation:

$$Q = \rho \cdot Q_v \cdot c_p \cdot \Delta T \tag{4}$$

Assuming a cabinet heat generation $Q = 12$ kW and a temperature rise $\Delta T = 10$°C, the required air volume Q_v is calculated to be 1 m³/s.

To maintain a safety margin, a fan system with a total airflow of several thousand CFM is required for the power supply cabinet. The existing heat dissipation configuration, featuring 2 air intake fans and 4 exhaust fans, fails to meet the cooling requirements of the absorption circuit.

DESIGN AND SIMULATION OF ENERGY FEEDBACK CIRCUIT

Pulse sources utilizing absorption circuits suffer from low energy utilization efficiency and challenging heat dissipation. To address these issues, this paper proposes a novel energy feedback unit that recycles energy, previously dissipated in the absorption circuit, back to the energy storage capacitor for reuse in next current pulse generation.

As shown in Fig. 3(a), a discharge diode connected in series with the discharge switch ensures only forward current flows through the discharge circuit, suppressing the underdamped impact energy following the first current pulse and

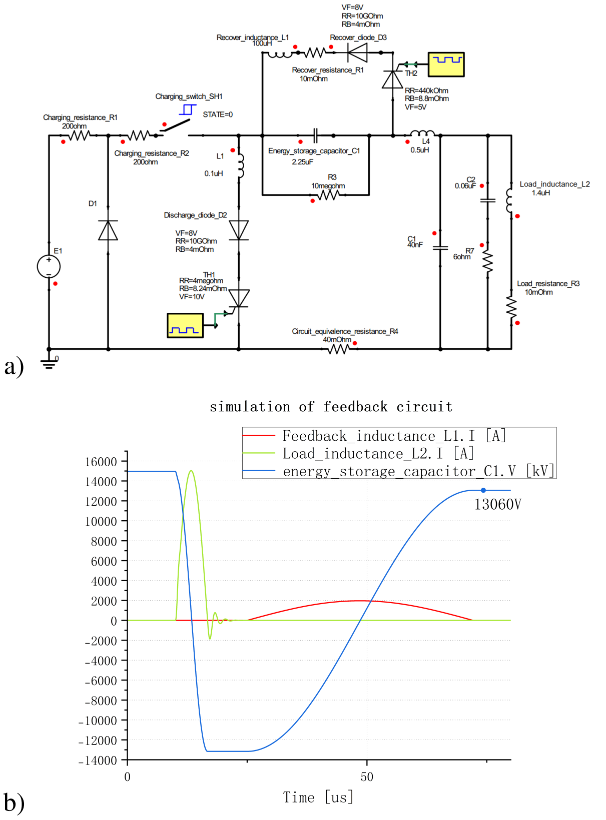

Figure 3: Simulation of the feedback circuit. (a) Simulation diagram. (b) Simulated results.

storing this energy in the capacitor as reverse voltage. After the discharge switch returns to the cut-off state, the feedback switch will be activated, forming an energy feedback circuit with the energy storage capacitor and feedback inductor.

A 100 uH feedback inductor was paired with the energy storage capacitor. The simulation result of corresponding capacitor voltage and main circuit currents are presented in Fig. 3. After the energy feedback process of each pulse, the energy storage capacitor voltage is restored to 13 kV in the forward direction, with 190 J of energy fed back to the capacitor. The implementation of the feedback circuit reduces the energy required to recharge the capacitor per discharge cycle, decreasing input power by 75% .

With the energy feedback circuit, Cabinet heat generation is reduced from 12 kW (with the absorption circuit) to 2.5 kW. Using Eq. (4) and assuming $\Delta T = 10$°C, the required fan air volume Q_v is calculated to be only 0.2 m³/s.

To maintain a safety margin, four 388 CFM exhaust fans were installed on the cabinet top for heat dissipation. Additionally, a water cooling system was adopted for critical semiconductor components.

Simulations of the cabinet internal heat dissipation were conducted, with the temperature results presented in Fig. 4. Under an ambient temperature of 20°C, the maximum surface temperature of components in the main discharge circuit is 33.6°C, and the maximum surface temperature of components in the energy feedback circuit is approximately 30°C,

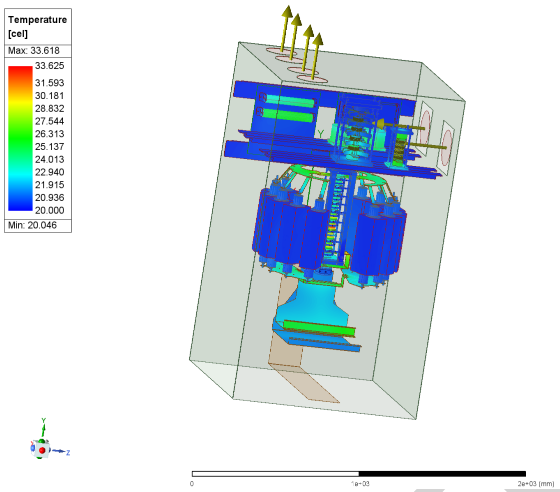

Figure 4: Heat dissipation simulation of cabinet interior.

both of which are within the safe operating temperature range.

CONCLUSION

This study addresses the critical challenges of high energy loss and severe heat dissipation in the 15 kV/15 kA AMD excitation pulse source for the STCF positron source, through the design and simulation of an energy feedback circuit integrated with novel photoconductive semiconductor switches.

This energy feedback design significantly improves the energy efficiency and long-term operational stability of the AMD excitation pulse source. Future work will focus on fabricating a prototype to validate the simulation results, optimizing the voltage-sharing circuit of series-connected photoconductive thyristors to enhance switch reliability. The proposed energy feedback architecture can also be generalized to other high-current pulse power systems in accelerators, offering a scalable approach to mitigate energy consumption and heat dissipation challenges in high-energy physics facilities.

REFERENCES

[1] J. Bao *et al.*, “Conceptual design report of the super tau-charm facility: the accelerator”, *Nucl. Sci. Tech.*, vol. 36, no. 12, p. 242, 2025. doi:10.48550/arXiv.2509.11522

[2] Q. Luo *et al.*, “The new progress in injector and positron source of STCF”, *Mod. Phys. Lett. A*, vol. 39, no. 40, p. 2440003, 2024. doi:10.1142/S0217732324400030

[3] J. Liu, “Research on the flux concentrator and its solid-state pulse power system for intense positron source”, Ph.D. thesis, University of Science and Technology of China, 2021. doi:10.27517/d.cnki.gzkju.2021.002485

[4] H. Bajas, S. Doebert, A. Latina, and Y. Zhao, “Flux concentrator optimization for future positron sources”, *IEEE Trans. Appl. Supercond.*, vol. 32, no. 6, pp. 1–5, 2022. doi:10.1109/TASC.2022.3160405

[5] F. Shang, “Study of a novel dual-channel kicker and its excitation solid-state pulse power supply for HALF”, Ph.D. thesis, University of Science and Technology of China, 2024. doi:10.27517/d.cnki.gzkju.2024.001024

[6] M.-n. Lin *et al.*, “Prototype of repetitive pulsed power supply for the RCS beam extraction kicker in the CSNS upgrade”, *Nucl. Instrum. Methods Phys. Res. A*, vol. 1061, p. 169146, 2024. doi:10.1016/j.nima.2024.169146